Anomalous Thermal Expansion of Cuprites: A Combined High Resolution Pair Distribution Function and Geometric Analysis

Karena W. Chapman* and Peter J. Chupas*

X-ray Science Division, Advanced Photon Source, Argonne National Laboratory, Argonne, Illinois 60439

Received October 24, 2008

The temperature-dependent local structures of cuprites (M_2O for M = Cu^I, Ag^I) have been probed using variable-temperature (80−500 K) high-resolution pair distribution function (PDF) analysis of X-ray scattering data measured to very high values of momentum transfer (Q_{max} = 35 $Å^{-1}$). These noble metal oxides exhibit negative thermal expansion (NTE) behavior; however, several unusual structural features and behaviors distinguish the cuprites from other NTE frameworks—the structure is inverted relative to conventional NTE frameworks and Cu_2O (but not Ag_2O) shows an unusual transition from negative to positive thermal expansion behavior at higher temperature—thus motivating the present in-depth analysis of the particular thermal expansion mechanisms operating here. By coupling the local structural information from the PDFs with known geometric identities of the tetrahedra that form the framework, distortions contributing to NTE have been identified and the contrasting high temperature behaviors of the two isostructural analogues have been accounted for. Specifically, we demonstrate that thermal population of low-energy vibrational modes involving the dynamic distortion of the OM_4 tetrahedra, away from the *regular* tetrahedral geometry (through M−O−M′ bending), can induce a contraction of the average tetrahedral edge length (M···M′) and thus contribute to the NTE effect. This mechanism operates in combination with the transverse vibrational mechanism found in conventional NTE frameworks, where increasing transverse displacement of the bridging atom (O−M−O′) draws corner-bridged polyhedra closer together.

Introduction

The discovery of materials that exhibit negative thermal expansion (NTE) behavior that persists over a wide temperature range has generated considerable interest, due in part to the valuable technological applications of such materials in moderating the positive thermal expansion (PTE) behavior of "normal" materials. Once thought to be a rare materials property, NTE behavior has now been documented in a range of materials including in a number of oxide-based frameworks (e.g., AM_2O_8,[1−3] AM_2O_7,[4,5] $A_2M_3O_{12}$,[6] NASICON,[7] MO_3,[8] M_2O,[9] and zeolites)[10] and more recently in more extended frameworks formed by cyanide (e.g., $M(CN)_2$,[11−13] Prussian blues)[14−16] or organic linkages (i.e., metal−organic frameworks).[17−21] In such framework systems, the NTE phenomenon is generally attributed to the thermal population of low-energy transverse vibrations of the ditopic bridging unit (single, double, or multiple atom) which draws the corner-linked polyhedra closer together to give a bulk NTE despite the PTE of individual bonds. This mechanism has been supported by structural[22,13] and computational studies of selected systems.[23,24]

Among NTE materials, the cuprite family of noble metal oxides (M_2O), for which NTE behavior has been reported in the Cu and Ag analogues, is particularly interesting.[9,25−30] Although not ostensibly dissimilar to other NTE frameworks formed by corner-linked polyhedra, including related systems

* Corresponding author. E-mail: chapmank@aps.anl.gov, chupas@anl.gov.

(1) Martinek, C.; Hummel, F. A. *J. Am. Ceram. Soc.* **1968**, *51*, 227–228.
(2) Mary, T. A.; Evans, J. S. O.; Vogt, T.; Sleight, A. W. *Science (Washington, D. C.)* **1996**, *272*, 90–92.
(3) Lind, C.; Wilkinson, A. P.; Hu, Z. B.; Short, S.; Jorgensen, J. D. *Chem. Mater.* **1998**, *10*, 2335–2337.
(4) Taylor, D. *Br. Ceram. Trans. J.* **1988**, *87*, 39–45.
(5) Korthuis, V.; Khosrovani, N.; Sleight, A. W.; Roberts, N.; Dupree, R.; Warren, W. W. *Chem. Mater.* **1995**, *7*, 412–417.
(6) Evans, J. S. O.; Mary, T. A.; Sleight, A. W. *J. Solid State Chem.* **1997**, *133*, 580–583.
(7) Roy, R.; Agrawal, D. K.; McKinstry, H. A. *Annu. Rev. Mater. Sci.* **1989**, *19*, 59–81.
(8) Tao, J. Z.; Sleight, A. W. *J. Solid State Chem.* **2003**, *173*, 45–48.
(9) Taylor, D. *Br. Ceram. Trans. J.* **1985**, *84*, 9–14.
(10) Lightfoot, P.; Woodcock, D. A.; Maple, M. J.; Villaescusa, L. A.; Wright, P. A. *J. Mater. Chem.* **2001**, *11*, 212–216.
(11) Williams, D. J.; Partin, D. E.; Lincoln, F. J.; Kouvetakis, J.; O'Keeffe, M. *J. Solid State Chem.* **1997**, *134*, 164–169.
(12) Goodwin, A. L.; Kepert, C. J. *Phys. Rev. B* **2005**, *71*, 140301.
(13) Chapman, K. W.; Chupas, P. J.; Kepert, C. J. *J. Am. Chem. Soc.* **2005**, *127*, 15630–15636.
(14) Margadonna, S.; Prassides, K.; Fitch, A. N. *J. Am. Chem. Soc.* **2004**, *126*, 15390–15391.
(15) Chapman, K. W.; Chupas, P. J.; Kepert, C. J. *J. Am. Chem. Soc.* **2006**, *128*, 7009–7014.
(16) Goodwin, A. L.; Chapman, K. W.; Kepert, C. J. *J. Am. Chem. Soc.* **2005**, *127*, 17980–17981.
(17) Rowsell, J. L. C.; Spencer, E. C.; Eckert, J.; Howard, J. A. K.; Yaghi, O. M. *Science (Washington, D. C.)* **2005**, *309*, 1350–1354.
(18) Dubbeldam, D.; Walton, K. S.; Ellis, D. E.; Snurr, R. Q. *Angew. Chem., Int. Ed.* **2007**, *46*, 4496–4499.
(19) Wu, Y.; Kobayashi, A.; Halder, G. J.; Peterson, V. K.; Chapman, K. W.; Lock, N.; Southon, P. D.; Kepert, C. J. *Angew. Chem., Int. Ed.* **2008**, *47*, 8929−8932.
(20) Han, S. S.; Goddard, W. A. *J. Phys. Chem. C* **2007**, *111*, 15185–15191.
(21) Zhou, W.; Wu, H.; Yildirim, T.; Simpson, J. R.; Walker, A. R. H. *Phys. Rev. B* **2008**, *78*, 054114.
(22) Tucker, M. G.; Goodwin, A. L.; Dove, M. T.; Keen, D. A.; Wells, S. A.; Evans, J. S. O. *Phys. Rev. Lett.* **2005**, *95*, 255501.
(23) Heine, V.; Welche, P. R. L.; Dove, M. T. *J. Am. Ceram. Soc.* **1999**, *82*, 1793–1803.

10.1021/cm802900t CCC: $40.75
Published on Web 01/02/2009

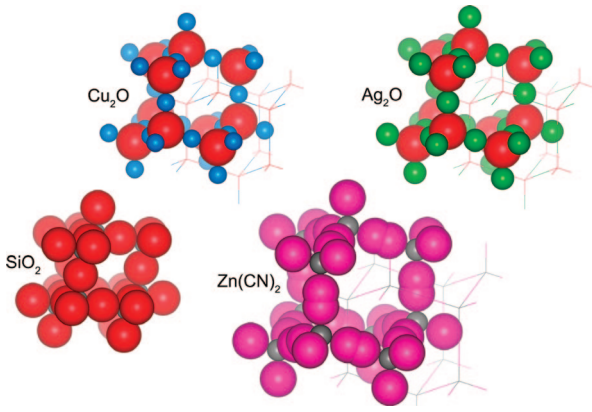

Figure 1. Space-filling representations of the cuprites Cu_2O and Ag_2O, β-cristobalite (SiO_2), and zinc cyanide ($Zn(CN)_2$) structures, which share the **dia** topology, reflecting the relevant ionic sizes. For clarity, one of the interpenetrated networks for the cuprites and zinc cyanide has been represented in outline form.

for which the NTE mechanism has been studied in depth, a number of unusual structure features and behaviors are unique to the cuprites. These call into question the validity of simply extending the established transverse vibrational mechanism for NTE to this family.

The cubic framework (M_2O, $Pn\bar{3}m$) can be considered as four-coordinate O^{2-} centers bridged linearly by two-coordinate M(I) to form doubly interpenetrated diamondoid networks (**dia** topology) of corner-sharing OM_4 tetrahedra.[31,32] The O−M−O connectivity with bridging Ag(I)/Cu(I) ions is inverted relative to other NTE frameworks where the bridging atoms are exclusively lightweight, hard-electron donors such as O^{2-} (or CN^-) with M−O−M (or M−CN−M) connectivity. As such, the M_2O cuprites are the only NTE framework materials for which the metal is the bridging atom.[33,34] The **dia** topology of the cuprite systems is shared by several low and negative thermal expansion oxide- and cyanide-bridged systems (Figure 1), including zinc cyanide ($Zn(CN)_2$, expanded anticuprite) and β-cristobalite (SiO_2, noninterpenetrated anticuprite). The more open network structure in cuprite and $Zn(CN)_2$ allows the interpenetration of an identical, independent network.

Within the isostructural cuprite family, there are not only quantitative differences in thermal expansion behavior[15] but also contrasting qualitative behaviors: Ag_2O remains NTE at all temperatures, while Cu_2O only exhibits NTE behavior at low temperature (>200 K), becoming less NTE and eventually PTE at high temperature. While a general reduction in the magnitude of NTE at high temperatures is to be expected—low-energy modes which contribute to NTE may become saturated and/or higher-energy modes associated with PTE may become more significantly populated—such a NTE-PTE crossover is virtually unknown in other systems.[35]

As the only NTE material with the heavier M cations bridging and with an unusual NTE−PTE crossover, an independent in-depth analysis of the mechanism underlying the thermal expansion behavior in the cuprite family is warranted.

Recently, the pair distribution function (PDF) method has emerged as a powerful technique for studying the local structural mechanism underlying the NTE effect,[13,22] including in $Zn(CN)_2$. The PDF method probes the local bond lengths and distances, which can deviate from those in the average, crystallographically determined structure, thus providing insight into the dynamic structural distortions. Here, we use high resolution PDF analysis of X-ray scattering data to probe the temperature dependence of the local structure in the cuprites Cu_2O and Ag_2O. The apparent simplicity of the cuprite structure, with a monatomic bridging and a single type of coordination polyhedra, masks a complex local structural problem with overlapping inter- and intranetwork correlations. By coupling high-resolution information from the PDF (Q_{max} = 35 Å^{-1}) on the temperature dependence of the local atomic distances that define the coordination polyhedra, with known geometric identities of the tetrahedron, it has been possible to identify structural distortions contributing to the NTE behavior and account for the contrasting high-temperature behaviors of the two isostructural analogues.

Experimental Methods

High-energy X-ray scattering data were collected at the 1-ID-C beamline of the Advanced Photon Source at Argonne National Laboratory. Using incident X-ray energies of 128.016 keV (λ = 0.09865 Å) in combination with a highly sensitive amorphous silicon-based area detector from General Electric Healthcare,[23] with 2048 × 2048 pixels covering a 41 × 41 cm active area, data were collected to high values of momentum transfer, $Q = 4\pi \sin(\theta/\lambda)$.[36,37] Powdered samples of Cu_2O (Aldrich, 99.99%) and Ag_2O (Aldrich, 99.99%) in polyimide capillaries were aligned in the X-ray beam. The sample temperature was controlled using an Oxford Cryosystems Cryostream 700 Plus and data were collected at 5 K intervals upon continuous heating at 100 K h^{-1} from 80 to 500 K. The sample-to-detector distance and tilt of the detector relative to the beam were refined within Fit-2D based on an image obtained for a LaB_6 NIST standard. The raw images were reduced within Fit-2D to obtain one-dimensional diffraction data (Q vs intensity).[38,39]

(24) Giddy, A. P.; Dove, M. T.; Pawley, G. S. *Acta Crystallogr., Sect. A* **1993**, *A49*, 697–703.
(25) Schafer, W.; Kirfel, A. *Appl. Phys. A: Mater. Sci. Proc.* **2002**, *74*, S1010−S1012.
(26) Dapiaggi, M.; Tiano, W.; Artioli, G.; Sanson, A.; Fornasini, P. *Nucl. Instrum. Methods Phys. Res., Sect. B* **2003**, *200*, 231–236.
(27) Tiano, W.; Dapiaggi, M.; Artioli, G. *J. Appl. Crystallogr.* **2003**, *36*, 1461–1463.
(28) Kennedy, B. J.; Kubota, Y.; Kato, K. *Solid State Commun.* **2005**, *136*, 177–180.
(29) Artioli, G.; Dapiaggi, M.; Fornasini, P.; Sanson, A.; Rocca, F.; Merli, M. *J. Phys. Chem. Solids* **2006**, *67*, 1918–1922.
(30) Sanson, A.; Rocca, F.; Dalba, G.; Fornasini, P.; Grisenti, R.; Dapiaggi, M.; Artioli, G. *Phys. Rev. B* **2006**, *73*, 214305.
(31) Niggli, P. *Z. Kristallogr.* **1922**, *57*, 253–299.
(32) Wyckoff, R. W. G. *Am. J. Sci.* **1922**, *3*, 184–188.
(33) Oxides with the delafossite structure, containing O−Cu/Ag−O linkages have been shown to have low-temperature NTE along a single crystallographic axis parallel to the O−Cu/Ag−O direction. See, for example, Li, J.; Yokochi, A.; Amos, T. G.; Sleight, A. W. *Chem. Mater.* **2002**, *14*, 2602–2606.
(34) Li, J.; Sleight, A. W.; Jones, C. Y.; Toby, B. H. *J. Solid State Chem.* **2005**, *178*, 285–294.
(35) In oxides with the delafossite structure, the low-temperature uniaxial NTE switches to being strongly PTE at high temperature.
(36) Chupas, P. J.; Qiu, X.; Hanson, J. C.; Lee, P. L.; Grey, C. P.; Billinge, S. J. L. *J. Appl. Crystallogr.* **2003**, *36*, 1342–1347.
(37) Chupas, P. J.; Chapman, K. W.; Lee, P. L. *J. Appl. Crystallogr.* **2007**, *40*, 463–470.

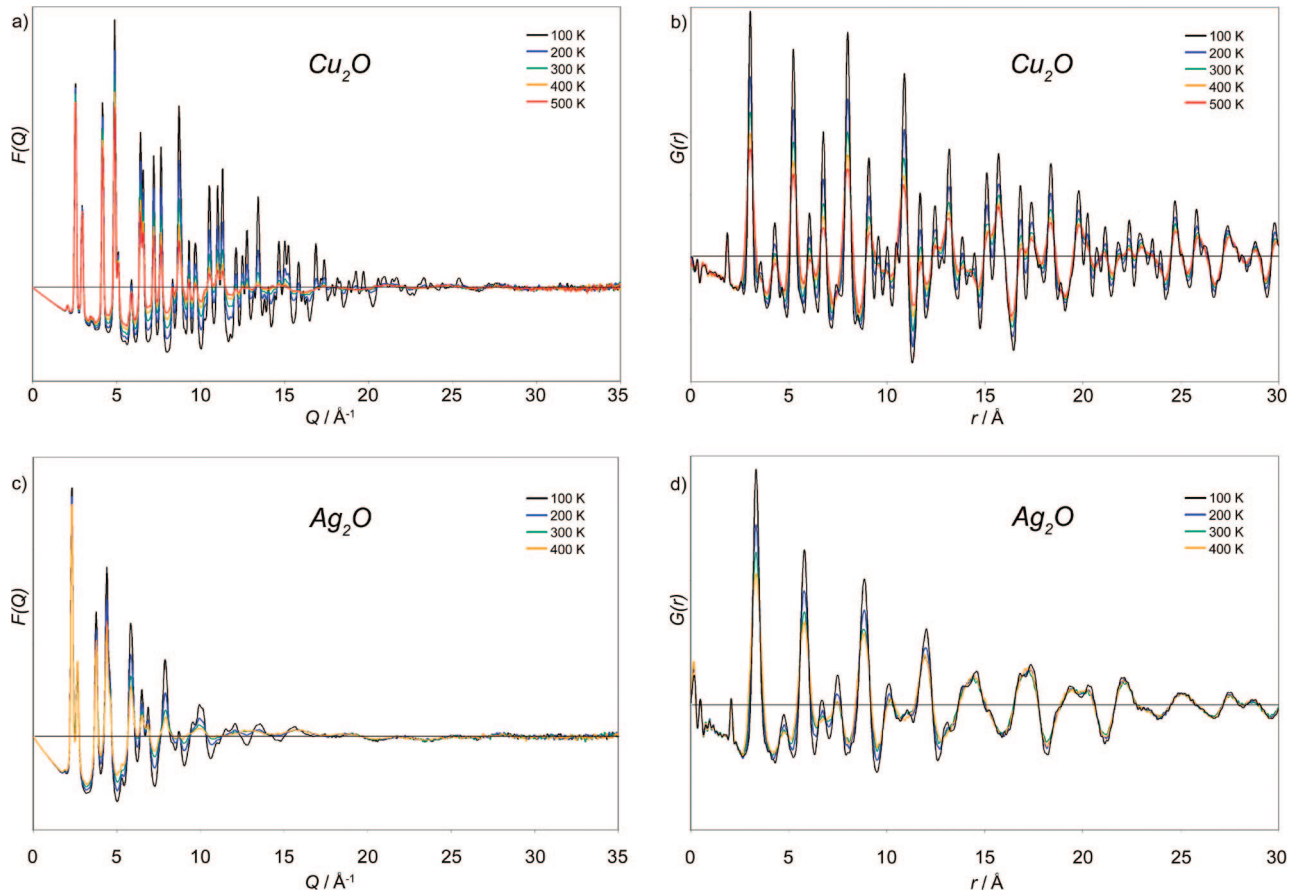

Figure 2. Selected temperature-dependent reduced structure functions, $F(Q)$, and PDFs, $G(r)$, obtained for Cu_2O and Ag_2O.

The PDFs $G(r) = 4\pi r[\rho(r) - \rho_o]$ where $\rho(r)$ and ρ_o are the instantaneous and average densities were extracted using PDFgetX2,[40] subtracting the contributions from the sample environment and background to the measured diffraction intensities. Corrections for multiple scattering, X-ray polarization, sample absorption, and Compton scattering were then applied to obtain the structure function $S(Q)$. Direct Fourier transform of the reduced structure function $F(Q) = Q[S(Q) - 1]$ up to $Q_{max} = 35$ Å^{-1} gave $G(r)$, the pair distribution function. Interatomic distances of interest were evaluated directly from the PDFs by fitting Gaussian functions to the peaks at ~1.86 Å (d_{Cu-O}), ~2.08 Å (d_{Ag-O}), ~3.02 Å ($d_{Cu\cdots Cu}$) and ~3.34 Å ($d_{Ag\cdots Ag}$). Refinement of a structural model and lattice parameter against $G(r)$ and generation of partial PDFs were performed within PDFFIT.[41]

Results

Representative temperature-dependent $F(Q)$'s and the corresponding PDFs, $G(r)$, obtained for the cuprite phases are shown in Figure 2. For Cu_2O, the PDFs contain sharp features to large distances as is consistent with the long-range crystallographic order of the system. Similar features are evident in the PDFs of the Ag analogue, although these are noticeably broader at all temperatures, suggesting a greater degree of static (nonthermal) disorder, and are shifted to longer distances consistent with the larger Ag^I cation and Ag_2O lattice parameter.

For Cu_2O, the general features in the PDF, beyond the nearest-neighbor Cu−O peak, broaden continuously with increasing temperature. While this broadening appears to be uniform up to 30 Å for Cu_2O, intriguingly for Ag_2O only the short-range correlations (<12 Å) broaden visibly with temperature. The initially broad longer-range features—the aggregates of multiple distinct correlations (i.e., individual peaks) of similar length—remain relatively invariant. This suggests that in Ag_2O there is a degree of medium-range static disorder on length scales of *ca.* 12Å, with a more ordered short-range structure.

The low-r peaks in the PDFs at ~1.86 Å and ~2.07 Å correspond to the nearest-neighbor M−O distance within OM_4 tetrahedra, for Cu and Ag, respectively (Figure 3). The average Cu−O and Ag−O bond lengths increase approximately linearly at similar rates upon heating (Figure 4). The bond length coefficients of thermal expansion (CTEs, $\alpha_l = dl/(l\,dT)$) are comparable to that observed using PDF methods for the Zn−C/N bond in the related $Zn(CN)_2$ phase[13] but are quite different from those based on extended X-ray absorption fine structure (EXAFS) studies of the local M environments,[30] in which α_{O-Cu} was reported to be 35% lower and α_{O-Ag} ~300% higher, than found for the present data (see Table 1). Although a greater CTE for O−Ag compared to O−Cu is consistent with the longer (i.e., weaker) bond, a factor of 4−5 increase in CTE suggested by EXAFS may be larger than expected for a ~0.2

(38) Hammersley, A. P. European Synchrotron Radiation Facility Internal Report, ESRF97HA02T; 1997.
(39) Hammersley, A. P.; Svensson, S. O.; Hanfland, M.; Fitch, A. N.; Häusermann, D. *High Pressure Res.* **1996**, *14*, 235–248.
(40) Qiu, X.; Thompson, J. W.; Billinge, S. J. L. *J. Appl. Crystallogr.* **2004**, *37*, 678.
(41) Proffen, T.; Billinge, S. J. L. *J. Appl. Crystallogr.* **1999**, *32*, 572–575.

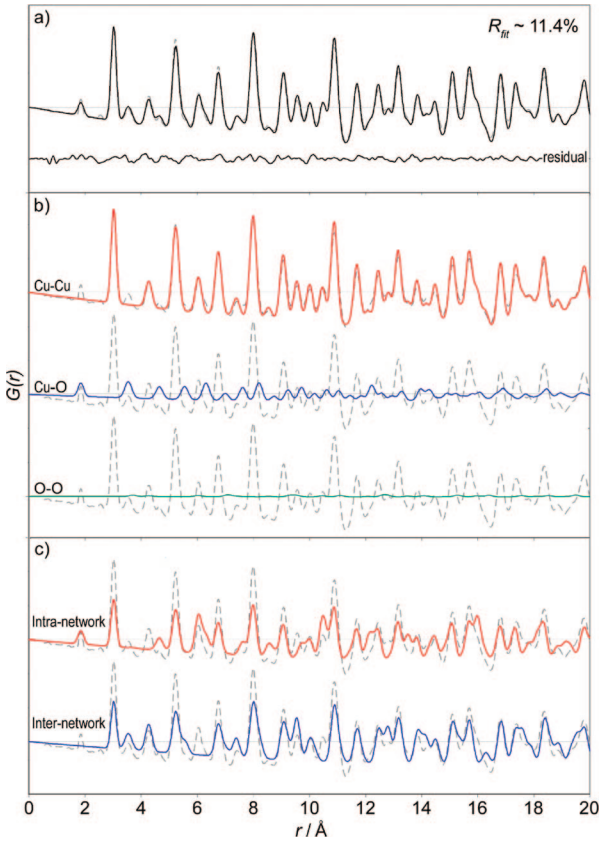

Figure 3. (a) PDF of Cu_2O calculated for a model, based on the crystal structure, fit to the data at 100 K and the corresponding residual to the fit. The associated partial PDFs corresponding to the interatomic (b) and inter/intra-network (c) correlations. The experimental PDF (dashed) is provided for reference.

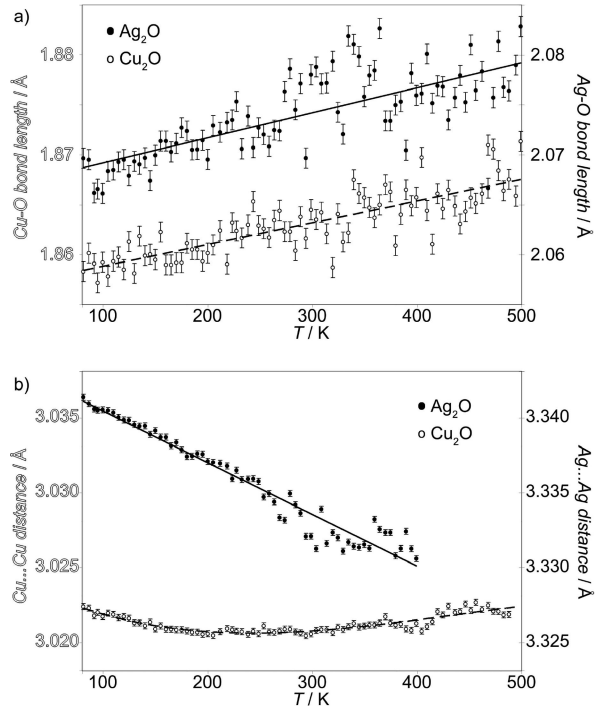

Figure 4. Temperature-dependent bond lengths and distances in Cu_2O and Ag_2O. Least-squares fits to the data of straight lines and polynomial ($d_{Cu\cdots Cu'}$) are shown. The greater relative intensity of the M···M′ correlation allows this distance to be determined with greater precision from the PDF than the M−O correlation.

Table 1. Coefficients of Thermal Expansion for the Nearest-Neighbor Bond Lengths Found Here and in Related dia **Structures**

bond	d (100 K), Å	α, (× 10^{-6}) K^{-1}	method
Si−O	1.62	+2.2(4)	PDF[42]
Zn−C/N	2.02	+10.2(10)	PDF[13]
O−Cu	1.86	+11.7(9)	PDF
O−Ag	2.07	+12.1(12)	PDF
O−Cu	1.85	+7.5	EXAFS[30]
O−Ag	2.05	+35	EXAFS[30]

Table 2. Coefficients of Thermal Expansion of M···M′ Distances

distance	T, K	α, (× 10^{-6}) K^{-1}
Cu···Cu′	80−180	−5.18(34)
Cu···Cu′	320−500	+2.8(4)
Ag···Ag′	80−250	−9.99(20)
Cu_2O	80	−5.4
Cu_2O	500	+2.8
Ag_2O	80	−7.0

Å difference in bond length. Although the Gaussian functions fit to determine the local bond lengths here do not allow for possible asymmetry of the peaks (as fit for the EXAFS data) there were no obvious peak asymmetries or peak shape changes in the present PDF data beyond a minor increase in peak width (d_{Cu-O}: by ca. 4% per 100 K; d_{Ag-O}: by ca. 8% per 100 K). As such, different peak fitting routines are unlikely to be the source of the different bond length CTEs. It is possibly that the differences in the CTEs are sample related, with defects being known to influence phase transition behavior in these phases.[30,28] Alternatively, difficulties in accurately modeling multiple-scattering effects in the EXAFS data may affect the extracted bond lengths and, accordingly, the CTEs.

The more intense peaks at ~3.02 Å and ~3.33 Å correspond to two chemically distinct M···M′ correlations: an *inter*network correlation along the edge of the OM_4 tetrahedral units and an *inter*network correlation between the (O)−M−(O′) bridges of different networks. In the average (crystallographic) structure, where the M ions are located on special positions, both types of M···M′ distances are constrained by symmetry to be identical. However, local deviations from the average structure may allow for different, distinct local M···M′ distances and thermal expansion behaviors.

At low temperatures, the average M···M′ next-nearest-neighbor distances contract with increasing temperature (Table 2). For Ag_2O, the contraction continues until the thermal reduction of Ag_2O above 400 K, with Ag···Ag′ correlations of similar length in the metallic Ag^0 product, preventing the reliable extraction of this distance. The Ag−O peak position and corresponding bond length remains unaffected by this reduction, although the peak intensity decreases progressively. In contrast, the Cu···Cu′ distance becomes progressively less NTE eventually becoming PTE at temperatures above ~240 K.

The thermal expansion of the lattice, from Rietveld refinement of the diffraction data, parallels the temperature dependence of the average next-nearest-neighbor M···M′

(42) Tucker, M. G.; Dove, M. T.; Keen, D. A. *J. Phys.: Condens. Matter* **2000**, *12*, L425−L430.

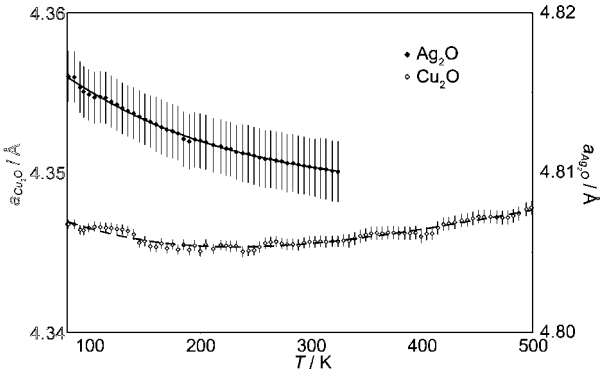

Figure 5. Temperature dependent lattice parameters for Cu_2O and Ag_2O.

distance (Figure 5). The errors in the lattice parameters reflect the necessarily low 2θ resolution afforded by an experimental configuration optimized for high Q_{max} and high real-space resolution measurements (with short wavelength X-rays and small sample-to-detector distance).

Discussion

At the low-temperature limit, where dynamic distortions of the structure are minimized (assuming little static disorder), the local atomic structure of the cuprites can be expected to converge to the average, long-range crystal structures, with linear O−M−O bridging and *regular* tetrahedral OM_4 geometry.[43]

According to the transverse vibrational mechanism characteristic of other NTE frameworks, the thermal population of low-energy modes involving the displacement of the bridging atom(s) away from the bridging axis—in this case, the displacement of the M away from the O···O′ axis—could induce a contraction of the tetrahedral centers in the cuprites and contribute to the NTE. While this effect could be directly observed using PDF methods in $Zn(CN)_2$, where the correlation between tetrahedral Zn centers was well resolved, due to the inverted nature of the cuprite structure, with the lightweight O atoms bridged by more strongly scattering M atoms, this effect is more difficult to probe here. Specifically, the X-ray PDF data are dominated by correlations involving the M atoms with comparatively low intensity O···O′ correlations.[44] However, the X-ray PDF data are particularly sensitive to the face-centered cubic sublattice of bridging/vertex M atoms and the nearest-neighbor O−M distance; accordingly, in the cuprites we can study fundamentally different aspects of the structure. These include the flexibility of the polyhedra and any correlated motion of the interpenetrated networks.

From the PDF data, the temperature dependence of the local next-nearest-neighbor M···M′ distances closely reflect the bulk thermal expansion of the lattice, with remarkable quantitative agreement:[45] The Ag···Ag′ distance contracts monotonically upon heating, while the Cu···Cu′ initially contracts before it expands on further heating. This similarity suggests that the mechanism underlying the overall thermal expansion behavior may be linked to the behavior of the local M···M′ distances. However, the considerable broadening of the M···M′ peak with temperature suggests a distribution of behaviors, and as such, the underlying mechanism cannot be straightforwardly defined from the data without broader consideration of the structure.

The M···M′ peak broadening likely reflects different temperature-dependent behaviors of chemically distinct intranetwork (vertex−vertex) and internetwork (bridge−bridge) M···M′ correlations, which precisely overlap in the crystal structure.

Consider first the OM_4 unit within the M_2O cuprite structure associated with the intranetwork M···M′ correlation. The metal ions define the vertices of a general tetrahedron that encloses the O atom. Within this tetrahedron, the PDF data confirm that the M−O distance (d_{M-O}) expands upon heating, as expected for directly bonded atom pairs. This expansion is approximately linear, with similar rates for both analogues. As such, an increasing PTE contribution from the M−O bond in Cu_2O at higher temperatures is unlikely to cause the striking NTE to PTE crossover observed. Furthermore, the particularly minor changes in peak widths suggest that all M−O bonds behave similarly.

According to the rigid-unit mode (RUM) model of NTE,[46,47,23] the M···M′ distance within the tetrahedron would be expected to be invariant with temperature. RUMs have been used to visualize how transverse vibrational motion in NTE frameworks are correlated through the lattice, through the relative rotation and translation of rigid units, with a large number of RUMs often associated with a large NTE effect. It considers polyhedra in framework structures to be rigid based on the approximation that vibrational modes which distort the polyhedra are of significantly higher energy, and therefore less populated, than lattice modes in which the polyhedra remain unchanged. While rigid-unit-type modes have been identified for frameworks with **dia** topology,[48,49,12] the rigid-unit approximation may be less valid here than for the oxide-based systems for which RUMs were originally conceived. For example, in SiO_2 systems such as β-cristobalite, a *regular* tetrahedral geometry maximizes the separation of the O-vertices[50,51] around the smaller Si^{IV} center ($r_O \sim$ 140 pm cf. $r_{Si} \sim 41$ pm)[52] such that distortion from this geometry is sterically unfavorable. In the OM_4 tetrahedra,

(43) In the *regular* tetrahedron, all faces are equilateral triangles and all edges are of the same length.

(44) The enhanced sensitivity to the M centers is comparable to EXAFS studies, although PDF data are not limited to the first few coordination shells, are not subject to multiple scattering artifacts, and yield atomic distances directly, i.e., are not derived using a structural model.

(45) By contrast, in the crystallographic structure, with all atoms on special positions, the thermal expansion of all interatomic distances are constrained to be identical to the lattice expansion.

(46) Tautz, F. S.; Heine, V.; Dove, M. T.; Chen, X. J. *Phys. Chem. Miner.* **1991**, *18*, 326–336.
(47) Pryde, A. K. A.; Hammonds, K. D.; Dove, M. T.; Heine, V.; Gale, J. D.; Warren, M. C. *J. Phys.: Condens. Matter* **1996**, *8*, 10973–10982.
(48) Swainson, I. P.; Dove, M. T. *Phys. Chem. Miner.* **1995**, *22*, 61–65.
(49) Hammonds, K. D.; Dove, M. T.; Giddy, A. P.; Heine, V.; Winkler, B. *Am. Mineral.* **1996**, *81*, 1057–1079.
(50) Chakerian, G. D.; Klamkin, M. S. *Am. Math. Mon.* **1973**, *80*, 1009–1017.
(51) Apostol, T. M.; Mnatsakanian, M. A. *Am. Math. Mon.* **2003**, *110*, 516–526.
(52) Shannon, R. D.; Prewitt, C. T. *Acta Crystallogr., Sect. B* **1970**, *26*, 1046–1048.

the relative sizes of the central and vertex atoms are inverted such that distortions of the tetrahedra, involving changes in the tetrahedral bond angle, may be significantly less sterically hindered than for MO_4 tetrahedra. Such compositional variability in the flexibility of polyhedral units has been demonstrated for zeotypes.[53,54] Consequently, the tetrahedra in the cuprites are likely to have enhanced flexiblity such that the RUMs model for NTE may be less appropriate.[55]

Due to the anticipated enhanced flexibility of the OM_4 tetrahedral units in cuprites, the temperature-dependence of the vertex−vertex M···M′ distance and the effect of tetrahedral distortions on the thermal expansion behavior must be explicitly considered. A property of tetrahedra is for tetrahedra inscribed on a given sphere, the maximum total (and average) edge length occurs for the *regular* tetrahedron.[50,51,56] As such, for a constant *circumradius/circumsphere*,[57] distortions of tetrahedra away from the regular geometry are associated with a reduction of the average edge length. The present high resolution PDF data on the cuprites show a relative invariance of the M−O peak width, which indicates a single M−O distance within each OM_4 tetrahedron. That is, the O lies at the centroid of the tetrahedron (and circumsphere), with circumradius equal to the length of the M−O bond. Consequently, increasing dynamic distortions of the OM_4 units from the *regular* tetrahedral geometry found at the low temperature extreme through variations of the central M−O−M′ angles (i.e., bending not stretching modes) will reduce the average vertex−vertex M···M′ distance.[58] Due to the enhanced flexibility of the tetrahedra, these modes would be expected to be of relatively low energy such that increasing thermal population of such modes and the associated contraction of the vertex−vertex M···M′ distance, can contribute to the observed NTE effect. The contraction of the vertex−vertex M···M′ distance with increasing temperature is consistent with models derived from EXAFS data.[30]

Thus, deviation from the RUM model through distortion of the polyhedra does not necessarily preclude the existence of low energy NTE modes. While the quasi-RUM extension to the RUM model allows for very small deformation of the rigid units (i.e., quasi-rigid units) to permit otherwise frustrated, relatively low-energy lattice modes, we have shown that dynamic distorting unit modes can be a separate mechanism contributing to NTE. Such modes are likely to play an important role in the NTE behavior of metal−organic frameworks, where the often expanded polyhedral units are likely to have enhanced flexibility.[19]

As the intranetwork M···M′ correlation is linked to an NTE effect, the high temperature PTE in Cu_2O must be associated with a strong PTE contribution from the internetwork bridge−bridge correlations—a contribution only activated at high temperatures above 200 K.

Charge density and computational investigations of the unusual M(I) coordination in the cuprites suggest that the predominately ionic bonding is accompanied by a degree of weak (internetwork) M···M′ interactions that stabilize the linear M(I) connectivity.[59−65] These closed-shell $d(10)-d(10)$ metallophilic intermolecular interactions, more often evident in molecular systems,[66−68] are typically associated with short cation−cation M···M′ distances of the order of those found in the cuprite structure. The relatively weak nature of such interactions is associated with a particularly broad interatomic potential, a greater bond length expansion upon thermal population of higher-amplitude vibrational modes, and accordingly a large PTE effect. Recently, a strong PTE effect associated with metallophilic (Ag···Ag′) interactions has been found to produce colossal anisotropic thermal expansion in flexible lattices, with the colossal positive thermal expansion coupled to an equally pronounced contraction in the perpendicular direction.[69,70] Moreover, such internetwork interactions may effectively couple the interpenetrated networks and lattice vibrations, to dampen or reduce the number of independent lattice modes (degrees of freedom) contributing to NTE.

In Cu_2O, the Cu atoms in the low-temperature structure may be sufficiently separated such that the cuprophilic interactions are negligible. On heating, the Cu cations are brought into closer proximity—through the overall lattice contraction and the increasing vibrational amplitudes of the Cu vertices/bridges—increasing the relevance of the cuprophilic interactions. These multiple effects account for the relatively abrupt onset of the PTE crossover.[71] In

(53) Zwijnenburg, M. A.; Cora, F.; Bell, R. G. *J. Am. Chem. Soc.* **2007**, *129*, 12588–12589.
(54) Zwijnenburg, M. A.; Huenerbein, R.; Bell, R. G.; Cora, F. *J. Solid State Chem.* **2006**, *179*, 3429–3436.
(55) Based on the relative ratios of the center-vertex atom size (see Figure 1), the tetrahedral flexibility in **dia** systems may be expected to be decrease $Cu_2O > Ag_2O \gg Zn(CN)_2 \gg SiO_2$.
(56) "The square of the sum of the edge lengths of any simplex in *m*-space is less than or equal to the number of edges times the sum of squares of the lengths of its edges, with equality if and only if the simplex is regular."[51]
(57) The *circumsphere* is the sphere containing the tetrahedron that passes through each of the vertices. The radius of this sphere is known as the *circumradius*.
(58) In the case of the regular tetrahedron vertex−vertex M···M′ distance, $d_{M\cdots M'}$, is given by $d_{M\cdots M'} = {}^2/_3\sqrt{6} \times d_{M-O} \approx 1.633 \times d_{M-O}$. This represents an upper bound for the vertex−vertex M···M′ distance. For a fixed radius (i.e. M−O distance), increasing distortion from *regular* tetrahedral geometry, through M−O−M′ bending modes, induces a contraction of the average tetrahedral edge length.
(59) Zuo, J. M.; Kim, M.; O'Keeffe, M.; Spence, J. C. H. *Nature* **1999**, *401*, 49–52.
(60) Wang, S. G.; Schwarz, W. H. E. *Angew. Chem., Int. Ed.* **2000**, *39*, 1757–1762.
(61) Zuo, J. M.; O'Keeffe, M.; Kim, M.; Spence, J. C. H. *Angew. Chem., Int. Ed.* **2000**, *39*, 3791–3794.
(62) Wang, S. G.; Schwarz, W. H. E. *Angew. Chem., Int. Ed.* **2000**, *39*, 3794–3796.
(63) Laskowski, R.; Blaha, P.; Schwarz, K. *Phys. Rev. B* **2003**, *67*, 075102.
(64) Filippetti, A.; Fiorentini, V. *Phys. Rev. B* **2005**, *72*, 035128.
(65) Gordienko, A. B.; Zhuravlev, Y. N.; Fedorov, D. G. *Phys. Solid State* **2007**, *49*, 223–228.
(66) Che, C. M.; Mao, Z.; Miskowski, V. M.; Tse, M. C.; Chan, C. K.; Cheung, K. K.; Phillips, D. L.; Leung, K. H. *Angew. Chem., Int. Ed.* **2000**, *39*, 4084–4088.
(67) Schmidbaur, H. *Gold Bull.* **2000**, *33*, 3–10.
(68) Hermann, H. L.; Boche, G.; Schwerdtfeger, P. *Chem. Eur. J.* **2001**, *7*, 5333–5342.
(69) Goodwin, A. L.; Calleja, M.; Conterio, M. J.; Dove, M. T.; Evans, J. S. O.; Keen, D. A.; Peters, L.; Tucker, M. G. *Science (Washington, D. C.)* **2008**, *319*, 794–797.
(70) Goodwin, A. L.; Keen, D. A.; Tucker, M. G.; Dove, M. T.; Peters, L.; Evans, J. S. O. *J. Am. Chem. Soc.* **2008**, *130*, 9660–9661.
(71) Such metallophilic interactions have also been identified in delafossites, see Kandpal, H. C.; Seshadri, R. *Solid State Sci.* **2002**, *4*, 1045–1052 (a similar mechanism may underlie the NTE-PTE crossover in those systems).

Ag_2O where the Ag atoms are more separated due the larger lattice, this effect is not apparent (at temperatures below decomposition, ca. 400 K).

Conclusion

We have delineated a novel mechanism for NTE involving the dynamic distortion of regular polyhedral units. This is compatible with the transverse vibrational mechanism established for conventional NTE materials. However, contrary to the RUM model which considers the vibration of bridging atoms about a common polyhedral center to be perfectly correlated such that the polyhedra remain unchanged, here, vibrations about a common polyhedral center are uncorrelated (or anticorrelated) such that the polyhedra are dynamically distorted—a dynamic-unit mode. Increasing amplitudes of distortions from the regular polyhedral geometry induces a contraction of the average polyhedral edge length (i.e., bridge−bridge distance) and thus contributes to the NTE behavior. This is in addition to the NTE contribution associated with the transverse vibrational motion of the bridging atoms which draws the connected polyhedral centers closer together (the sole mechanism in the RUM model).

In the cuprites, the OM_4 tetrahedra can be considered to be more tolerant to distortion than polyhedra in conventional NTE materials, based on the straightforward consideration of the relative ion size. As such the dynamic-unit modes would be of lower energy and would be likely to have a more significant thermal population.

The abrupt transition from negative to positive thermal expansion in Cu_2O upon heating is consistent with our proposed mechanism, with interactions between the interpenetrated networks—including cuprophilic interactions between bridging Cu cations—becoming more pronounced at high temperature. The larger lattice in Ag_2O minimizes the impact of such internetwork interaction such that NTE behavior is retained at all temperatures studied.

It is anticipated that similar high-resolution PDF studies will provide valuable insights into the thermal expansion in a variety of other materials, including in metal−organic framework materials.

Acknowledgment. Work performed at Argonne and use of the Advanced Photon Source were supported by the U.S. Department of Energy, Office of Science, Office of Basic Energy Sciences, under Contract No. DE-AC02-06CH11357.

CM802900T